

IDENTIFYING LATENT CAUSAL CONTENT FOR MULTI-SOURCE DOMAIN ADAPTATION

Yuhang Liu¹, Zhen Zhang¹, Dong Gong², Mingming Gong³, Biwei Huang⁴,
Kun Zhang⁵, Javen Qinfeng Shi¹

¹ Australian Institute for Machine Learning, The University of Adelaide, Australia

² School of Computer Science and Engineering, The University of New South Wales, Australia

³ School of Mathematics and Statistics, The University of Melbourne, Australia

⁴ Halicioğlu Data Science Institute (HDSI), University of California San Diego, USA

⁵ Department of Philosophy, Carnegie Mellon University, USA

yuhang.liu01@adelaide.edu.au

ABSTRACT

Multi-source domain adaptation (MSDA) learns to predict the labels in target domain data, under the setting where all data from multiple source domains are labelled and the data from the target domain are unlabeled. To handle this problem, most of methods focus on learning invariant representations across domains. However, their success severely relies on the assumption that label distribution remains unchanged across domains. To mitigate it, we propose a new assumption, *latent covariate shift (LCS)*, where the marginal distribution of the latent content variable changes across domains, and the conditional distribution of the label given the latent content remains invariant across domains. We introduce a latent style variable to complement the latent content variable forming a latent causal graph as the data and label generating process. We show that although the latent style variable is unidentifiable due to transitivity property in the latent space, the latent content variable can be identified up to simple scaling under some mild conditions. This motivates us to propose a novel method for MSDA, which learns the invariant label distribution conditional on the latent content variable, instead of learning invariant representations. Empirical evaluation on simulation and real data demonstrates the effectiveness of the proposed method, compared with many state-of-the-art methods based on invariant representation.

1 INTRODUCTION

Traditional machine learning requires the training and testing set to be independent and identically distributed distributions (Vapnik, 1999). This strict condition may not be fulfilled in various potential real-world applications. For example, in medical applications, it is common to seek to train a model on patients from few hospitals, and generalize it to a new hospital (Zech et al., 2018). In this case it is often reasonable to consider that the distributions of data from training hospitals are different from the new hospital (Koh et al., 2021). Domain adaptation (DA) is a promising research area to handle such problems. In general, DA can frequently be considered in multi-source settings (MSDA) where source domain data are collected from multiple domains. Formally, let \mathbf{x} denote the input, *e.g.* image, \mathbf{y} denote the labels in source and target domains, and \mathbf{D} denote the domain index. We observe labeled data pairs $(\mathbf{x}^S, \mathbf{y}^S)$ from the multiple joint distributions $p(\mathbf{x}, \mathbf{y}|\mathbf{D}_1), p(\mathbf{x}, \mathbf{y}|\mathbf{D}_2), \dots, p(\mathbf{x}, \mathbf{y}|\mathbf{D}_M)$ in source domains, and unlabeled input data \mathbf{x}^T from the joint distribution $p(\mathbf{x}, \mathbf{y}|\mathbf{D}_T)$ in target domain. The training phase of MSDA is to use $(\mathbf{x}^S, \mathbf{y}^S)$ and \mathbf{x}^T , to train a predictor so that it can provide a satisfactory estimation for \mathbf{y}^T in the target domain. The key for MSDA is to understand how the joint distribution change across different domains, resulting in $p(\mathbf{x}, \mathbf{y}|\mathbf{D}_1) \neq p(\mathbf{x}, \mathbf{y}|\mathbf{D}_2) \dots \neq p(\mathbf{x}, \mathbf{y}|\mathbf{D}_M) \neq p(\mathbf{x}, \mathbf{y}|\mathbf{D}_T)$.

Most early methods assume the change of the joint distribution results from *Covariate Shift* (Huang et al., 2006; Bickel et al., 2007; Sugiyama et al., 2007; Wen et al., 2014), *e.g.*, $p(\mathbf{x}, \mathbf{y}|\mathbf{D}_i) = p(\mathbf{y}|\mathbf{x})p(\mathbf{x}|\mathbf{D}_i)$, as depicted by Figure 1(a). This setting assumes that $p(\mathbf{x})$ changes across do-

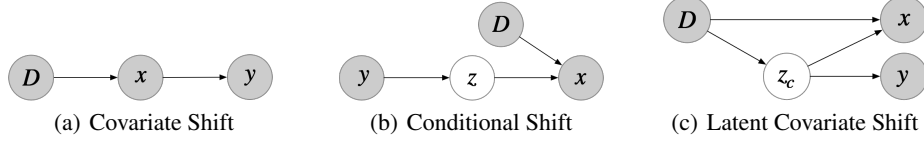


Figure 1: The illustration of three different assumptions for MSDA.

mains, while the conditional distribution $p(y|x)$ is invariant across domain. Such assumption is too strong for some real applications, especially for image data. For example, the assumption of invariant $p(y|x)$ implies that $p(y)$ should change as the change of $p(x)$. However, we can easily change style information in image data that is irrelevant to the label (e.g., background, view), so that the distribution $p(x)$ changes while the distribution of $p(y)$ remains unchanged, which clearly violates the assumption.

In contrast to covariate shift above, most current works consider a more reasonable assumption, *Conditional Shift* as depicted by Figure 1(b). It assumes that $p(x|y)$ changes while the distribution $p(y)$ is invariant across domains (Zhang et al., 2013; 2015; Schölkopf et al., 2012; Stojanov et al., 2021; Peng et al., 2019). This setting motivates a popular class of methods focusing on learning invariant representations across different domains to approach the true z in Figure 1(b) (Ganin et al., 2016; Zhao et al., 2018; Saito et al., 2018; Mancini et al., 2018; Yang et al., 2020; Wang et al., 2020; Li et al., 2021; Stojanov et al., 2021). However, the label distribution $p(y)$ may change across domains in many real application scenarios (Tachet des Combes et al., 2020; Lipton et al., 2018; Zhang et al., 2013). In these scenarios, those methods based on learning invariant representations, may be resulting in degenerating performance. In fact, recent work has proven an upper bound on the performance of those methods when label distributions change across domains (Zhao et al., 2019).

To relieve the problem above, this work proposes a new assumption, *Latent Covariate Shift (LCS)*, as depicted by Figure 1(c). Unlike to conditional shift, LCS assumes that there is a latent content variable z_c , whose marginal distribution $p(z_c)$ is variant across domains, and the label distribution conditional on it $p(y|z_c)$ is invariant. Due to the change of $p(z_c)$ across domains, LCS allows label distribution $p(y)$ to change across domain, due to the invariant $p(y|z_c)$. To more deeply understand and handle LCS, we propose a latent causal graph to formulate data and label generating process, by using two latent variables, e.g., the latent content variable z_c and the latent style variable z_s as depicted in Figure 2. In the proposed latent causal graph, the domain variable D causes the independent exogenous variables n_c and n_s , which are corresponding to the latent content variable z_c and the latent style variable z_s , respectively. The observed input data is caused by both z_c and z_s , while label is only caused by z_c . We show that although it is often impossible to identify the latent style variable z_s without strong assumptions, due to *transitivity property* in latent space, the latent content variable z_c can be identifiable up to simple scaling by using the identifiability result from nonlinear ICA (Khemakhem et al., 2020) and dependence between n_c and y . This motivates us to propose a novel method to learn the invariant conditional distribution $p(y|z_c)$ for MSDA, instead of learning invariant representations conditional on label. Since z_c is identifiable, the proposed method provides a principled way to guarantee that the learned predictor $p(y|z_c)$ can be generalized to the target domain. Empirical evaluation on synthetic and real data demonstrates the effectiveness of the proposed method, compared with many state-of-the-art methods.

2 RELATED WORK

Learning invariant representations. Due to the strong assumptions in covariate shift, most current works for domain adaptation consider conditional shift, which learns invariant representations across domains (Ganin et al., 2016; Zhao et al., 2018; Saito et al., 2018; Mancini et al., 2018; Yang et al., 2020; Wang et al., 2020; Li et al., 2021). Such representations can be obtained by applying suitable linear or nonlinear transformation on the input data. The key of these methods is how to enforce the invariance of the learned representations. For example, the invariance can be enforced by maximum classifier discrepancy (Saito et al., 2018), or by a domain discriminator for adversarial training (Ganin et al., 2016; Zhao et al., 2018), or by moment matching (Peng et al., 2019), or by

relation alignment loss (Wang et al., 2020). However, all these methods assume label distribution to be invariant across domains. As a result, when label distribution is varying across domains, they may perform well only in the overlapping areas among the all label distributions in different domains, and face with challenges in the non-overlapping areas. To overcome this, some works propose to learn invariant representations conditional on the label across domains (Gong et al., 2016; Ghifary et al., 2016; Tachet des Combes et al., 2020). One of the challenges in these methods is that the labels in the target domain is unavailable. More importantly, these methods does not guarantee that the learnt representations to be consistent with the true relevant information for predicting the label in the target domain, thus there is no principled way to guarantee that the learned predictor can be generalized to the target domain.

Learning invariant conditional distribution $p(y|z_c)$. There exist few of works exploring the invariant conditional distribution $p(y|z_c)$ for domain adaptation (Kull & Flach, 2014; Bouvier et al., 2019). Differ from these two works, the proposed method provides the identifiability of z_c , so that the learned $p(y|z_c)$ in this work can be generalized to the target domain in a principled way. Besides, in the context of out-of-distribution generalization, some recent works explore learning invariant conditional distribution $p(y|z_c)$ (Arjovsky et al., 2019; Sun et al., 2021; Liu et al., 2021; Lu et al., 2021). For example, Arjovsky et al. (2019) imposes learn the optimal invariant predictor across domains from the viewpoint of an intimate link between invariance and causation, while the proposed method directly explores conditional invariance given the proposed latent causal graph. Sun et al. (2021) mainly focus on single domain, while the proposed method consider multiple domains. The proposed method is also different from the work in Liu et al. (2021) in that the former assume the latent content variable caused by the style variable, while the latter depends on a confounder to model the causal relation between the latent content variable and the style variable. Unlike the work in Lu et al. (2021) that the label is treated as a variable causing the other latent variables, the proposed method assumes that the label have no child nodes.

3 THE PROPOSED LATENT CAUSAL GRAPH FOR LATENT COVARIATE SHIFT

To more deeply understand and handle LCS, we introduce a latent causal graph as depicted by Figure 2. It introduces the observed domain variable D to denote in which specific domain data are collected. Let n_c and n_s denote the noise (exogenous) variables. According to the definition of structural causal model (Pearl, 2000; Spirtes et al., 2001), n_c and n_s should be mutually independent conditional on the observed D . Both n_c and n_s are corresponding to the latent content variable z_c and the latent style variable z_s , respectively. Here z_c and z_s denote the latent causal content information and the latent style information, respectively. Generally speaking, z_c and z_s should be dependent given the domain variable D . Here we consider that z_c causes z_s , to model the correlation between z_s and y . In the proposed latent causal graph, z_c change across domains while $p(y|z_c)$ is invariant across domains, which meets the basic assumption in latent covariate shift. In the following, we discuss two key causal relations, which also highlights the novelty of the proposed latent causal graph.

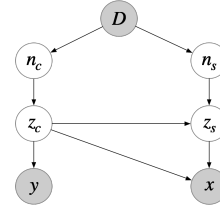


Figure 2: The proposed latent causal model.

z_c causes y : Previous works consider the causal relation between x and y as $y \rightarrow x$ (Gong et al., 2016; Stojanov et al., 2019; Li et al., 2018), while we employ $z_c \rightarrow y$. We argue that these two cases are not contradictory since the labels y in these two cases represent two different physical meanings. To understand this point, let \hat{y} replace y in the first case (i.e., $\hat{y} \rightarrow x$) to distinguish from y in the second case. For the first case, consider the generative process of images. A label should be first sampled, e.g., \hat{y} , then one may determine content information regarding to the label \hat{y} , and finally generate a image, which is a reasonable assumption in many real application scenarios. In the proposed latent causal graph, n_c play a role to replace \hat{y} and causes the content variable z_c . We then assume $z_c \rightarrow y$, which formulates the process that experts extract content information from given images and then provide reasonable labels according to their domain knowledge. This assumption has been made by some recent works (Mahajan et al., 2021; Liu et al., 2021; Sun et al.,

2021). Particularly, these two different labels, \hat{y} and y , has been considered in the work (Mahajan et al., 2021). Here we provide a further detailed interpretation for the difference between \hat{y} and y .

z_c causes z_s : It is clear that there exists a spurious correlation between the label y and the style variable z_s in many real applications. We here employ z_c as a confounding factor of both y and z_s to model the spurious correlation. The rationality of this assumption can be further verified from the viewpoint of the converse. In particular, if we assume that z_s causes z_c , all high-level information in input data x , z_s and z_c , would be causally related to the label y , which can not model the spurious correlation and is obviously unreasonable. Therefore, assuming $z_c \rightarrow z_s$ is more persuasive and consistent with previous works (Gong et al., 2016; Stojanov et al., 2019; Mahajan et al., 2021). One recent work in (Sun et al., 2021) leverages a additional variable as a confounding factor that causes both the content variable z_c and the style variable z_s to model their relation. However, the identifiability in the work (Sun et al., 2021) do not depend on the confounding factor. As a result, the confounding factor can be incorporated into the domain index, which is equivalent to the case where z_c and z_s are independent for a single domain. By contrast, the proposed latent graph assumes a more general setting where z_c and z_s are dependent for a single domain, as depicted by Figure 2. Experimental results will further highlight the advantages of the proposed latent causal graph, compared with the work (Sun et al., 2021).

4 IDENTIFIABILITY ANALYSIS OF THE PROPOSED LATENT CAUSAL GRAPH

In this section, we will show that z_c can be identifiable up to simple scaling under some mild conditions. To this end, we first provide some identifiable results in nonlinear ICA (Khemakhem et al., 2020), which shows that the exogenous variables, n_c and n_s , can be identifiable up to simple permutation and scaling with some mild conditions. With this result, we then show that although the proposed latent causal graph as a whole is unidentifiable due to *transitivity property*, the part of the graph z_c can also be identifiable up to simple scaling, by using the dependence between n_c and y .

4.1 IDENTIFYING n_c AND n_s UP TO PERMUTATION AND SCALING BY NONLINER ICA

Nonlinear ICA aims to separate independent latent variables, e.g., n_c and n_s , from observed mixing data, e.g., x , generated by a nonlinear function. It is known that nonlinear ICA is highly ill-posed, and one can not recover the independent latent variables, without some assumptions (Hyvärinen & Pajunen, 1999). Recent work in (Khemakhem et al., 2020) has show that under relatively mild conditions independent latent variables can be identifiable. Specifically, one can assume there is an auxiliary observed variable, similar as D in Figure 2, which influences the distributions of all independent latent variables. This auxiliary variable could be time series or side information. Conditioning on the auxiliary variable, we can recover the independent latent variables up to simple permutation and scaling. The auxiliary variable could also be regarded as domain index, and causes both n_c and n_s as depicted in Figure 2. In addition, the input data x can be regarded as observed mixing data. Since we can see all input data x from source and target domains in the setting of domain adaptation, it is trivial to extend the identifiability result of nonlinear ICA to the proposed causal graph, i.e., n_c and n_s in source and target domains can be recover up to simple permutation and scaling under the mild conditions. For example, independent latent variables n_s and n_c are sampled from independent Gaussian distributions whose means and variances are modulated by the observed variable D as mentioned in Khemakhem et al. (2020). Note that we here assume n_s and n_c to be vectors. Although the identifiability result of nonlinear ICA is prove for scalar, we assume all components in these two vectors to be mutually independent, which is reasonable because both vectors denote noise variables, so that the identifiability result of nonlinear ICA can also be used for n_s and n_c .

4.2 THE CURSE OF IDENTIFIABILITY IN LATENT SPACE: TRANSITIVITY PROPERTY

Even with the identifiability result of n_c and n_s , it is still challenging to completely identify the proposed causal graph. In fact, we have the following result:

Proposition 4.1. *With the identifiability result of n_c and n_s , the proposed causal graph is unidentifiable*

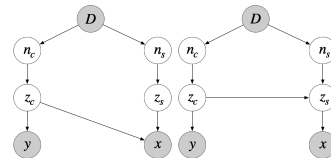


Figure 3: Two equivalent graph structures.

without additional assumptions, due to transitive property in latent space.

Proof. To prove non-identifiability, it is sufficient to show that several different graph structures lead to the same observed data. In particular, given the fact that \mathbf{n}_c and \mathbf{n}_s is identifiable up to permutation and scaling, let us consider the net effect of \mathbf{n}_c on \mathbf{x} . There are two different paths to 'explain' the net effect of \mathbf{n}_c on \mathbf{x} . One path is $\mathbf{n}_c \rightarrow \mathbf{z}_c \rightarrow \mathbf{x}$. In this case, since we have no limitation on the function class of edges, we can cut the path $\mathbf{z}_c \rightarrow \mathbf{z}_s$ off (e.g., the left sub-figure of Figure 3) and obtain the same observed data depicted by Figure 2. The other path is $\mathbf{n}_c \rightarrow \mathbf{z}_c \rightarrow \mathbf{z}_s \rightarrow \mathbf{x}$. In this case, we can cut the 'path' $\mathbf{z}_c \rightarrow \mathbf{x}$ off (e.g., the right sub-figure of Figure 3) and generate same observed data depicted by Figure 2. Therefore, two sub-figure are equivalent with the proposed latent causal graph in Figure 3. \square

The non-identifiability result above is because we can not determine which path is the correct path corresponding to the net effect of \mathbf{n}_c on \mathbf{x} , e.g., $\mathbf{n}_c \rightarrow \mathbf{z}_c \rightarrow \mathbf{x}$ or $\mathbf{n}_c \rightarrow \mathbf{z}_c \rightarrow \mathbf{z}_s \rightarrow \mathbf{x}$. We term it *transitivity property* in this work. It often appears in latent causal discovery and seriously hinders the identifiability. For reader who may be interested in that problem, we recommend recent work (Adams et al., 2021).

4.3 IDENTIFYING \mathbf{z}_c UP TO SCALING BY THE DEPENDENCE BETWEEN \mathbf{n}_c^S AND \mathbf{y}^S

Although the proposed causal graph as a whole is unidentifiable, for domain adaptation application we are only interested in the identifiability of \mathbf{z}_c , instead of the latent variable \mathbf{z}_s , since label \mathbf{y} is only caused by \mathbf{z}_c . Due to the observed \mathbf{y}^S from source domains, we have the following result:

Proposition 4.2. *With the assumptions of nonlinear ICA, the content variable \mathbf{z}_c in the proposed latent causal graph can be identifiable up to simple scaling by using the dependence between \mathbf{n}_c^S and \mathbf{y}^S from source domains.*

Proof. As mentioned above, there are permutation indeterminacy and scaling indeterminacy in identifying \mathbf{n}_c and \mathbf{n}_s . The permutation indeterminacy implies that if we obtain the two recovered variables, e.g., $\hat{\mathbf{n}}_c$ and $\hat{\mathbf{n}}_s$, we are uncertain of which the recovered variable is the latent content variable \mathbf{n}_c , i.e., $\mathbf{n}_c = \hat{\mathbf{n}}_c$ or $\mathbf{n}_c = \hat{\mathbf{n}}_s$. If we can solve this permutation problem, since the parent node of \mathbf{z}_c includes \mathbf{n}_c only, \mathbf{z}_c can also be identifiable up to scaling, i.e., $\mathbf{z}_c = f(\mathbf{n}_c)$ where f can be any nonlinear function. Let us consider the relationships among \mathbf{n}_c , \mathbf{n}_s and \mathbf{y} in the proposed causal graph, it is clear that the label \mathbf{y} only depends on \mathbf{n}_c and is independent with \mathbf{n}_s , given the domain variable \mathbf{D} . As a result, we can compute the correlations (e.g., by mutual information) between \mathbf{y}^S and $\hat{\mathbf{n}}_c^S$ or between \mathbf{y}^S and $\hat{\mathbf{n}}_s^S$, to determine which recovered variable is \mathbf{n}_c . Here superscript S denotes data from source domains. \square

The proposition shows that the content variable \mathbf{z}_c can be identifiable up to simple scaling. The scaling indeterminacy of \mathbf{z}_c is no significance and can be ignored in latent space, since this indeterminacy can be 'absorbed' by nonlinear function class of edges and do not change the causal direction. For example, consider the recovered variable $\hat{\mathbf{z}}_c$ and its scaling *scaling*($\hat{\mathbf{z}}_c$). When we try to learn a invariant predictor $g(\cdot)$ from $\hat{\mathbf{z}}_c$ to \mathbf{y} , the scaling indeterminacy can be 'absorbed' by a composition predictor, e.g., $g(\text{scaling}(\cdot))$.

5 LEARNING INVARIANT $p(\mathbf{y}|\mathbf{z}_c)$ FOR MSDA

The identifiable \mathbf{z}_c provides a principled way to guarantee that we can learn the conditional distribution $p(\mathbf{y}|\mathbf{z}_c)$ to be generalized to the target domain. In this section we propose a novel method to show how to learn the invariant conditional distribution $p(\mathbf{y}|\mathbf{z}_c)$ for MSDA.

5.1 THE PROPOSED METHOD FOR LEARNING INVARIANT $p(\mathbf{y}|\mathbf{z}_c)$

As mentioned in section 4.3, since the identifiability \mathbf{z}_c is built on the identifiability result of nonlinear ICA, we need to identify \mathbf{n}_c and \mathbf{n}_s first. To meet the conditions of identifiable \mathbf{n}_c and \mathbf{n}_s as

mentioned in Khemakhem et al. (2020), we employ the following Gaussian prior on \mathbf{n}_c and \mathbf{n}_s :

$$p(\mathbf{n}|\mathbf{D}) = p(\mathbf{n}_c|\mathbf{D})p(\mathbf{n}_s|\mathbf{D}) = \mathcal{N}(\boldsymbol{\mu}_{\mathbf{n}_c}(\mathbf{D}), \Sigma_{\mathbf{n}_c}(\mathbf{D}))\mathcal{N}(\boldsymbol{\mu}_{\mathbf{n}_s}(\mathbf{D}), \Sigma_{\mathbf{n}_s}(\mathbf{D})), \quad (1)$$

where $\boldsymbol{\mu}$ and Σ denote the mean and variance, respectively. Both are depending on the domain variable \mathbf{D} and can be implemented by multi-layer perceptrons. Since \mathbf{n}_c and \mathbf{n}_s could be vector and are corresponding to independent noise variables, Σ here is a diagonal matrix. There are some exponential distributions, *e.g.*, Laplace distribution, which also meets the conditions of identifiable \mathbf{n}_c and \mathbf{n}_s and thus are feasible (Khemakhem et al., 2020). We here employ the Gaussian prior since it is flexible to directly use the re-parametric trick (Kingma & Welling, 2013). The nature of the proposed Gaussian prior equation 1 gives rise to the following variational posterior:

$$q(\mathbf{n}|\mathbf{D}, \mathbf{x}) = q(\mathbf{n}_c|\mathbf{D}, \mathbf{x})q(\mathbf{n}_s|\mathbf{D}, \mathbf{x}) = \mathcal{N}(\boldsymbol{\mu}'_{\mathbf{n}_c}(\mathbf{D}, \mathbf{x}), \Sigma'_{\mathbf{n}_c}(\mathbf{D}, \mathbf{x}))\mathcal{N}(\boldsymbol{\mu}'_{\mathbf{n}_s}(\mathbf{D}, \mathbf{x}), \Sigma'_{\mathbf{n}_s}(\mathbf{D}, \mathbf{x})), \quad (2)$$

where $\boldsymbol{\mu}'$ and Σ' denote the mean and variance of the posterior, respectively. Again, both are depending on the domain variable \mathbf{D} and the observed \mathbf{x} , and can be implemented by multi-layer perceptrons. Combining this with the Gaussian prior equation 1, we arrive at the following evidence lower bound (ELBO):

$$\max \mathbb{E}_{q(\mathbf{n}|\mathbf{D}, \mathbf{x})}(p(\mathbf{x}|\mathbf{D})) - D_{\mathcal{KL}}(q(\mathbf{n}|\mathbf{D}, \mathbf{x})||p(\mathbf{n}|\mathbf{D})), \quad (3)$$

where $D_{\mathcal{KL}}$ denotes the Kullback–Leibler divergence.

Maximizing the ELBO equation 3, we can recover \mathbf{n}_c and \mathbf{n}_s up to simple scaling and permutation. To solve the permutation as mentioned in section 4.3, we can simultaneously maximize the dependence of \mathbf{y}^S and \mathbf{n}_c^S . Here we employ the mutual information to maximize the dependence. As a result, we arrive at:

$$\max \lambda \underbrace{(\mathbb{E}_{q(\mathbf{n}|\mathbf{D}, \mathbf{x})}(p(\mathbf{x}|\mathbf{D})) - D_{\mathcal{KL}}(q(\mathbf{n}|\mathbf{D}, \mathbf{x})||p(\mathbf{n}|\mathbf{D})))}_{ELBO} + \underbrace{I(\mathbf{n}_c^S, \mathbf{y}^S)}_{MI}, \quad (4)$$

where $I(\mathbf{n}_c^S, \mathbf{y}^S)$ denotes the mutual information between \mathbf{n}_c^S and \mathbf{y}^S in source domains. λ is a regularization hyper-parameter that balances the ELBO and the mutual information (MI). The proposed method is termed iLCC-MSDA (identifiable latent causal content for MSDA), includes two part, ELBO and mutual information. The ELBO ensures that \mathbf{n}_c and \mathbf{n}_s can be recovered up to scaling and permutation. The MI handles the permutation, and thus ensures the recovered \mathbf{n}_c to be corresponding to the true latent content variable, instead of the latent style variable. In the implementation, we use the variational low bound of mutual information proposed by Alemi et al. (2016) to approximate the mutual information in equation 4.

$$\max \lambda (\mathbb{E}_{q(\mathbf{n}|\mathbf{D}, \mathbf{x})}(p(\mathbf{x}|\mathbf{D})) - D_{\mathcal{KL}}(q(\mathbf{n}|\mathbf{D}, \mathbf{x})||p(\mathbf{n}|\mathbf{D}))) + \mathbb{E}_{q(\mathbf{n}_c|\mathbf{D}, \mathbf{x})}(p(\mathbf{y}^S|\mathbf{n}_c^S)). \quad (5)$$

A depiction of the proposed iLCC-MSDA is shown in Figure 4.

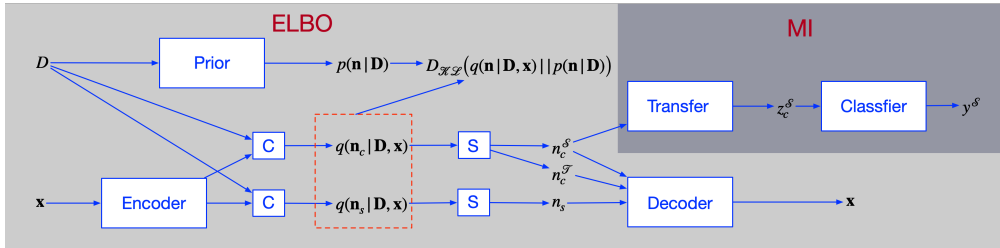


Figure 4: The proposed iLCC-MSDA to learn the invariant $p(\mathbf{y}^S|\mathbf{z}_c^S)$ for multiple source domain adaptation. C denotes concatenation, S denotes sampling from a distribution.

5.2 HEURISTIC CONSTRAINTS FOR THE PROPOSED METHOD

Enhancing the independence of \mathbf{n}_c and \mathbf{n}_s As we discussed, the performance of the proposed iLCC-MSDA above depends on the assumptions for the identifiability of \mathbf{n}_c and \mathbf{n}_s . For example,

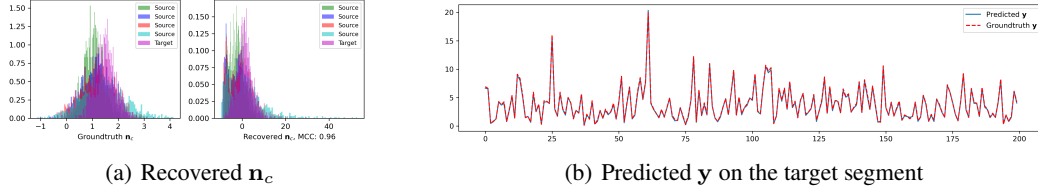


Figure 5: The Result on Synthetic Data.

one of the assumptions is that there exist many different domains to change the distributions of \mathbf{n}_c and \mathbf{n}_s . However, in practical implementation we may have no lots of source domains for domain adaptation in real applications. To remedy this, we employ a heuristic method to enhance the independence. Motivated by the progress in disentangled representation learning (Higgins et al., 2017; Kim & Mnih, 2018; Chen et al., 2018), we propose using a hyperparameter β to control the emphasis on learning statistically the independent latent variables \mathbf{n}_c and \mathbf{n}_s given the domain variable \mathbf{D} .

Entropy regularization In the loss function equation 5, we enforce the causal relation between \mathbf{y}^S and \mathbf{n}_c^S in source domains by the mutual information. To encourage such causal relation in target domain, we can also maximize the mutual information between \mathbf{y}^T and \mathbf{n}_c^T by minimizing the conditional entropy:

$$L_{ent} = -\mathbb{E}\left(p(\mathbf{y}|\mathbf{z}_c^T) \log p(\mathbf{y}|\mathbf{z}_c^T)\right) \quad (6)$$

This regularization has been empirically used in previous works (Wang et al., 2020; Li et al., 2021), while we consider it from the viewpoint of causality. Overall, our loss function is:

$$\max \lambda(\mathbb{E}_{q(\mathbf{n}|\mathbf{D}, \mathbf{x})}(p(\mathbf{x}|\mathbf{D})) - \beta D_{KL}(q(\mathbf{n}|\mathbf{D}, \mathbf{x})||p(\mathbf{n}|\mathbf{D}))) + \mathbb{E}_{q(\mathbf{n}_c|\mathbf{D}, \mathbf{x})}(p(\mathbf{y}^S|\mathbf{n}_c^S)) + \gamma L_{ent}, \quad (7)$$

where β, λ, γ are hyper-parameters that trade off the independence of \mathbf{n}_c and \mathbf{n}_s , the classifier and the entropy regularization loss terms.

6 EXPERIMENTS

6.1 EXPERIMENTS ON SYNTHETIC DATA

Dataset We conduct experiments on synthetic data, generated by the following process: we divide the latent variables into 5 segments, which are corresponding to 5 domains. Each segment includes 1000 examples. Within each segment, we first sample the mean and the variance from uniform distributions $[1, 2]$ and $[0.3, 1]$ for the latent exogenous variables \mathbf{n}_c and \mathbf{n}_s , respectively. Then for each segment, we generate $\mathbf{z}_c, \mathbf{z}_s, \mathbf{x}$ and \mathbf{y} according to the following structural causal model:

$$\mathbf{z}_c := \mathbf{n}_c, \quad \mathbf{z}_s := \mathbf{z}_c^3 + \mathbf{n}_s, \quad \mathbf{y} := \mathbf{z}_c^3, \quad \mathbf{x} := MLP(\mathbf{z}_c, \mathbf{z}_s), \quad (8)$$

where following (Khemakhem et al., 2020) we mix the latent \mathbf{z}_c and \mathbf{z}_s using a multi-layer perceptron to generate \mathbf{x} .

Results In implementation, we use the first 4 segments as source domains, and the last segment as target domain. Figure 5(a) shows the true and recovered distributions of the exogenous variables \mathbf{n}_c . Due to the support of nonlinear ICA, the proposed iLCC-MSDA obtain the mean correlation coefficient (MCC) 0.96 between the original \mathbf{n}_c and the recovered. Due to the invariant conditional distribution $p(\mathbf{y}|\mathbf{n}_c)$, even with the change of distribution of the exogenous variables \mathbf{n}_c as shown in Figure 5(a), the learned $p(\mathbf{y}|\mathbf{n}_c)$ can be generalized to target segment in a principle way as depicted by the Figure 5(b). Due to the limited space, Figure 5(b) only shows 200 samples for the true and predicted \mathbf{y} .

6.2 EXPERIMENTS ON REAL DATA

Dataset We further evaluate the proposed iLCC-MSDA on benchmark domain adaptation dataset PACS dataset (Li et al., 2017) and Terra Incognita (Beery et al., 2018). To obtaining the situation of

label distribution shift on PACS dataset, we filtered the original dataset by re-sampling it to generate three datasets, PACS ($D_{KL} = 0.3$), PACS ($D_{KL} = 0.5$) and PACS ($D_{KL} = 0.7$), where $D_{KL} = 0.3(0.5, 0.7)$ denotes that KL divergence is approximately 0.3 (0.5, 0.7) for label distributions of any two different domains. See Figure 6 for detailed label distributions.

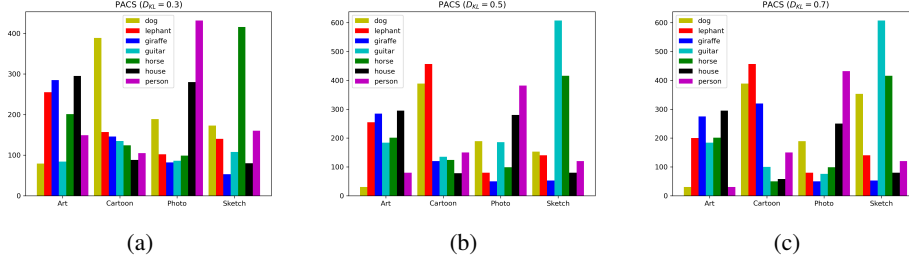


Figure 6: Label distributions of the filtered PACS data.

Baselines We compare the proposed method with state-of-the-art methods to verify its effectiveness. Particularly, we compare the proposed methods with empirical risk minimization (ERM), MCDA (Saito et al., 2018), M3DA (Peng et al., 2019), LtC-MSDA (Wang et al., 2020), T-SVDNet (Li et al., 2021), IRM (Arjovsky et al., 2019), IWCDAN (Tachet des Combes et al., 2020) and LaCIM (Sun et al., 2021). In these methods, MCDA, M3DA, LtC-MSDA and T-SVDNet learn an invariant representation, while IRM, IWCDAN and LaCIM learn invariant conditional distributions for MSDA, allowing label distribution to shift. Details of implementation, including network architectures and hyper-parameter setting, are in the APPENDIX. All the proposed methods are averaged over 3 runs with standard deviation.

Ablation studies The bottom of Table 1 and 2 presents the results for ablation studies. We can observe that entropy regularization equation 6 significantly increases the performance (around 10% and 5%) of the proposed method on both dataset. This justifies the importance of the causal relation between \mathbf{y} and \mathbf{n}_c , which is consistent with our model assumption. Besides, the hyper-parameter β also boosts the performance by enforcing the independence between the latent variables \mathbf{n}_c and \mathbf{n}_s .

Results The results by different methods on PACS are presented in Table 1. We can observe that as the increase of KL divergence of label distribution, the performance of MCDA, M3DA, LtC-MSDA and T-SVDNet, which are based on learning an invariant representations, gradually degenerates. When the KL divergence is about 0.7, the performance of these methods is worse than traditional ERM. Compared with the methods, which allows label distribution to change across domains, including IRM, IWCDAN and LaCIM, the proposed iLCC-MSDA obtains the best performance, due to our theoretical insights. Table 2 depicts the results by different methods on challenging Terra Incognit. The proposed iLCC-MSDA achieves a significant performance gain on the challenging task $\rightarrow L7$. Compared with the other methods, the proposed iLCC-MSDA is the only one that is superior to ERM.

7 CONCLUSION

The key for domain adaptation is understanding how the joint distribution of input data and label changes across domains. Previous works assume the covariate shift or the conditional shift to interpret the change of the joint distribution, which may be severely restricted in real applications. This work relaxes these assumptions and proposes a new assumption, latent covariate shift. To handle it, we propose a latent causal graph to more precisely formulate the generative process of input data and label, by using a latent causal variable and a latent style variables. Built on the identifiability result of nonlinear ICA, we show that the latent causal variable can be identified up to scaling. This motivates us a new method to learn invariant label distribution conditional on the latent causal variable, with a principled way to guarantee generalization. Experiments show the advantages of our

Table 1: Classification results and ablation study on PACS data.

PACS ($D_{KL} = 0.3$)					
Methods	Accuracy				
	→Art	→Cartoon	→Photo	→Sketch	Average
ERM	82.3 ± 0.3	81.3 ± 0.9	94.9 ± 0.2	76.2 ± 0.7	83.6
MCDA ((Saito et al., 2018))	76.6 ± 0.6	85.1 ± 0.3	96.6 ± 0.1	70.1 ± 1.3	82.1
M3SDA (Peng et al., 2019)	79.6 ± 1.0	86.6 ± 0.5	97.1 ± 0.3	83.3 ± 1.0	86.6
LtC-MSDA (Wang et al., 2020)	82.7 ± 1.3	84.9 ± 1.4	96.9 ± 0.2	75.3 ± 3.1	84.9
T-SVDNet (Li et al., 2021)	81.8 ± 0.3	86.5 ± 0.2	95.9 ± 0.2	80.7 ± 0.8	86.3
IRM (Arjovsky et al., 2019)	79.6 ± 0.7	77.0 ± 2.2	94.6 ± 0.2	71.7 ± 2.3	80.7
IWCDAN (Tachet des Combes et al., 2020)	84.0 ± 0.5	78.1 ± 0.7	96.0 ± 0.1	75.5 ± 1.9	83.4
LaCIM (Sun et al., 2021)	63.1 ± 1.5	72.6 ± 1.0	82.7 ± 1.3	71.5 ± 0.9	72.5
iLCC-MSDA(Ours)	86.4 ± 0.8	81.1 ± 0.8	95.9 ± 0.1	86.0 ± 1.0	87.4

PACS ($D_{KL} = 0.5$)					
Methods	Accuracy				
	→Art	→Cartoon	→Photo	→Sketch	Average
ERM	85.4 ± 0.6	76.4 ± 0.5	94.4 ± 0.4	85.0 ± 0.6	85.3
MCDA ((Saito et al., 2018))	81.6 ± 0.1	76.8 ± 0.1	93.6 ± 0.1	84.1 ± .6	84.0
M3SDA (Peng et al., 2019)	81.2 ± 1.2	77.5 ± 1.3	94.5 ± 0.5	84.3 ± 0.5	84.4
LtC-MSDA (Wang et al., 2020)	85.2 ± 1.5	75.2 ± 2.6	94.9 ± 0.6	85.1 ± 2.7	85.1
T-SVDNet (Li et al., 2021)	84.8 ± 0.3	77.6 ± 1.7	94.2 ± 0.2	86.4 ± 0.2	85.6
IRM (Arjovsky et al., 2019)	81.5 ± 0.3	71.1 ± 1.3	94.2 ± 0.1	78.7 ± 0.7	81.4
IWCDAN (Tachet des Combes et al., 2020)	79.2 ± 1.6	72.6 ± 0.7	95.6 ± 0.1	82.1 ± 2.2	82.4
LaCIM (Sun et al., 2021)	67.4 ± 1.6	66.6 ± 0.6	81.0 ± 1.2	82.3 ± 0.6	74.3
iLCC-MSDA(Ours)	89.0 ± 0.7	77.6 ± 0.5	95.0 ± 0.3	87.4 ± 1.6	87.3

PACS ($D_{KL} = 0.7$)					
Methods	Accuracy				
	→L28	→L43	→L46	→L7	Average
ERM	86.1 ± 0.6	76.8 ± 0.3	94.6 ± 0.4	81.3 ± 2.0	84.7
MCDA ((Saito et al., 2018))	80.8 ± 0.7	74.1 ± 1.2	94.4 ± 0.4	77.9 ± 0.4	81.8
M3SDA (Peng et al., 2019)	82.7 ± 1.3	76.2 ± 1.0	94.5 ± 0.7	80.8 ± 1.2	83.6
LtC-MSDA (Wang et al., 2020)	83.7 ± 1.6	74.6 ± 1.4	95.0 ± 0.7	80.8 ± 0.6	83.5
T-SVDNet (Li et al., 2021)	83.3 ± 0.8	74.7 ± 0.6	95.2 ± 0.3	74.5 ± 3.3	81.9
IRM (Arjovsky et al., 2019)	84.3 ± 0.8	73.3 ± 1.8	94.3 ± 0.1	69.4 ± 4.6	80.3
IWCDAN (Tachet des Combes et al., 2020)	76.3 ± 0.8	73.9 ± 1.6	93.1 ± 0.5	77.6 ± 3.8	80.2
LaCIM (Sun et al., 2021)	63.6 ± 0.9	68.7 ± 1.4	77.5 ± 3.8	77.8 ± 2.2	71.9
iLCC-MSDA(Ours)	90.7 ± 0.3	74.2 ± 0.7	95.8 ± 0.3	83.0 ± 2.2	86.0
iLCC-MSDA(Ours) with $\beta = 1$	90.2 ± 0.5	73.4 ± 0.8	95.7 ± 0.4	82.7 ± 0.7	85.5
iLCC-MSDA(Ours) with $\gamma = 0$	81.1 ± 1.5	70.0 ± 1.6	92.0 ± 0.5	59.6 ± 0.7	75.7

Table 2: Classification results on TerraIncognita.

Methods	Accuracy				
	→L28	→L43	→L46	→L7	Average
ERM	54.1 ± 2.8	62.3 ± 0.7	44.7 ± 0.9	74.5 ± 2.6	58.9
MCDA ((Saito et al., 2018))	54.9 ± 4.1	61.2 ± 1.2	42.7 ± 0.3	64.8 ± 8.1	55.9
M3SDA (Peng et al., 2019)	62.3 ± 1.4	62.7 ± 0.4	41.3 ± 0.3	57.4 ± 0.9	55.9
LtC-MSDA (Wang et al., 2020)	51.9 ± 5.7	54.6 ± 1.3	45.7 ± 1.0	69.1 ± 0.3	55.3
T-SVDNet (Li et al., 2021)	58.2 ± 1.7	61.9 ± 0.3	45.6 ± 2.0	68.2 ± 1.1	58.5
IRM (Arjovsky et al., 2019)	57.5 ± 1.7	60.7 ± 0.3	42.4 ± 0.6	74.1 ± 1.6	58.7
IWCDAN (Tachet des Combes et al., 2020)	58.1 ± 1.8	59.3 ± 1.9	43.8 ± 1.5	58.9 ± 3.8	55.0
LaCIM (Sun et al., 2021)	58.2 ± 3.3	59.8 ± 1.6	46.3 ± 1.1	70.8 ± 1.0	58.8
iLCC-MSDA(Ours)	64.3 ± 3.4	63.1 ± 1.6	44.7 ± 0.4	80.8 ± 0.4	63.2
iLCC-MSDA(Ours) with $\beta = 1$	56.3 ± 4.3	61.5 ± 0.7	45.2 ± 0.3	80.1 ± 0.6	60.8
iLCC-MSDA(Ours) with $\gamma = 0$	54.8 ± 1.4	58.9 ± 1.8	46.8 ± 1.4	73.1 ± 0.6	58.4

theoretical results and the performance of the the proposed method, compared with state-of-the-art methods across various dataset.

REFERENCES

- Jeffrey Adams, Niels Hansen, and Kun Zhang. Identification of partially observed linear causal models: Graphical conditions for the non-gaussian and heterogeneous cases. *Advances in Neural Information Processing Systems*, 34, 2021.
- Alexander A Alemi, Ian Fischer, Joshua V Dillon, and Kevin Murphy. Deep variational information bottleneck. *arXiv preprint arXiv:1612.00410*, 2016.
- Martin Arjovsky, Léon Bottou, Ishaan Gulrajani, and David Lopez-Paz. Invariant risk minimization. *arXiv preprint arXiv:1907.02893*, 2019.
- Sara Beery, Grant Van Horn, and Pietro Perona. Recognition in terra incognita. In *Proceedings of the European conference on computer vision (ECCV)*, pp. 456–473, 2018.
- Steffen Bickel, Michael Brückner, and Tobias Scheffer. Discriminative learning for differing training and test distributions. In *Proceedings of the 24th international conference on Machine learning*, pp. 81–88, 2007.
- Victor Bouvier, Philippe Very, Céline Hudelot, and Clément Chastagnol. Hidden covariate shift: A minimal assumption for domain adaptation. *arXiv preprint arXiv:1907.12299*, 2019.
- Ricky TQ Chen, Xuechen Li, Roger B Grosse, and David K Duvenaud. Isolating sources of disentanglement in variational autoencoders. *Advances in neural information processing systems*, 31, 2018.
- Yaroslav Ganin, Evgeniya Ustinova, Hana Ajakan, Pascal Germain, Hugo Larochelle, François Laviolette, Mario Marchand, and Victor Lempitsky. Domain-adversarial training of neural networks. *The journal of machine learning research*, 17(1):2096–2030, 2016.
- Muhammad Ghifary, David Balduzzi, W Bastiaan Kleijn, and Mengjie Zhang. Scatter component analysis: A unified framework for domain adaptation and domain generalization. *IEEE transactions on pattern analysis and machine intelligence*, 39(7):1414–1430, 2016.
- Mingming Gong, Kun Zhang, Tongliang Liu, Dacheng Tao, Clark Glymour, and Bernhard Schölkopf. Domain adaptation with conditional transferable components. In *International conference on machine learning*, pp. 2839–2848. PMLR, 2016.
- I. Higgins, Loïc Matthey, A. Pal, Christopher P. Burgess, Xavier Glorot, M. Botvinick, S. Mohamed, and Alexander Lerchner. beta-vae: Learning basic visual concepts with a constrained variational framework. In *ICLR*, 2017.
- Jiayuan Huang, Arthur Gretton, Karsten Borgwardt, Bernhard Schölkopf, and Alex Smola. Correcting sample selection bias by unlabeled data. *Advances in neural information processing systems*, 19, 2006.
- Aapo Hyvärinen and Petteri Pajunen. Nonlinear independent component analysis: Existence and uniqueness results. *Neural networks*, 12(3):429–439, 1999.
- Ilyes Khemakhem, Diederik Kingma, Ricardo Monti, and Aapo Hyvarinen. Variational autoencoders and nonlinear ica: A unifying framework. In *International Conference on Artificial Intelligence and Statistics*, pp. 2207–2217. PMLR, 2020.
- Hyunjik Kim and Andriy Mnih. Disentangling by factorising. In *International Conference on Machine Learning*, pp. 2649–2658. PMLR, 2018.
- Diederik P Kingma and Max Welling. Auto-encoding variational bayes. *arXiv preprint arXiv:1312.6114*, 2013.
- Pang Wei Koh, Shiori Sagawa, Henrik Marklund, Sang Michael Xie, Marvin Zhang, Akshay Bal-subramani, Weihua Hu, Michihiro Yasunaga, Richard Lanus Phillips, Irena Gao, et al. Wilds: A benchmark of in-the-wild distribution shifts. In *International Conference on Machine Learning*, pp. 5637–5664. PMLR, 2021.

- Meelis Kull and Peter Flach. Patterns of dataset shift. In *First International Workshop on Learning over Multiple Contexts (LMCE) at ECML-PKDD*, 2014.
- Da Li, Yongxin Yang, Yi-Zhe Song, and Timothy M Hospedales. Deeper, broader and artier domain generalization. In *Proceedings of the IEEE international conference on computer vision*, pp. 5542–5550, 2017.
- Ruihuang Li, Xu Jia, Jianzhong He, Shuaijun Chen, and Qinghua Hu. T-svdnet: Exploring high-order prototypical correlations for multi-source domain adaptation. In *Proceedings of the IEEE/CVF International Conference on Computer Vision*, pp. 9991–10000, 2021.
- Ya Li, Mingming Gong, Xinmei Tian, Tongliang Liu, and Dacheng Tao. Domain generalization via conditional invariant representations. In *Proceedings of the AAAI conference on artificial intelligence*, volume 32, 2018.
- Zachary Lipton, Yu-Xiang Wang, and Alexander Smola. Detecting and correcting for label shift with black box predictors. In *International conference on machine learning*, pp. 3122–3130. PMLR, 2018.
- Chang Liu, Xinwei Sun, Jindong Wang, Haoyue Tang, Tao Li, Tao Qin, Wei Chen, and Tie-Yan Liu. Learning causal semantic representation for out-of-distribution prediction. *Advances in Neural Information Processing Systems*, 34, 2021.
- Chaochao Lu, Yuhuai Wu, José Miguel Hernández-Lobato, and Bernhard Schölkopf. Invariant causal representation learning for out-of-distribution generalization. In *International Conference on Learning Representations*, 2021.
- Divyat Mahajan, Shruti Tople, and Amit Sharma. Domain generalization using causal matching. In *International Conference on Machine Learning*, pp. 7313–7324. PMLR, 2021.
- Massimiliano Mancini, Lorenzo Porzi, Samuel Rota Buló, Barbara Caputo, and Elisa Ricci. Boosting domain adaptation by discovering latent domains. In *Proceedings of the IEEE Conference on Computer Vision and Pattern Recognition*, pp. 3771–3780, 2018.
- J. Pearl. *Causality: Models, Reasoning, and Inference*. Cambridge University Press, Cambridge, 2000.
- Xingchao Peng, Qinxun Bai, Xide Xia, Zijun Huang, Kate Saenko, and Bo Wang. Moment matching for multi-source domain adaptation. In *Proceedings of the IEEE/CVF international conference on computer vision*, pp. 1406–1415, 2019.
- Kuniaki Saito, Kohei Watanabe, Yoshitaka Ushiku, and Tatsuya Harada. Maximum classifier discrepancy for unsupervised domain adaptation. In *Proceedings of the IEEE conference on computer vision and pattern recognition*, pp. 3723–3732, 2018.
- Bernhard Schölkopf, Dominik Janzing, Jonas Peters, Eleni Sgouritsa, Kun Zhang, and Joris Mooij. On causal and anticausal learning. *arXiv preprint arXiv:1206.6471*, 2012.
- P. Spirtes, C. Glymour, and R. Scheines. *Causation, Prediction, and Search*. MIT Press, Cambridge, MA, 2nd edition, 2001.
- Petar Stojanov, Mingming Gong, Jaime Carbonell, and Kun Zhang. Data-driven approach to multiple-source domain adaptation. In *The 22nd International Conference on Artificial Intelligence and Statistics*, pp. 3487–3496. PMLR, 2019.
- Petar Stojanov, Zijian Li, Mingming Gong, Ruichu Cai, Jaime Carbonell, and Kun Zhang. Domain adaptation with invariant representation learning: What transformations to learn? *Advances in Neural Information Processing Systems*, 34, 2021.
- Masashi Sugiyama, Shinichi Nakajima, Hisashi Kashima, Paul Buenau, and Motoaki Kawanabe. Direct importance estimation with model selection and its application to covariate shift adaptation. *Advances in neural information processing systems*, 20, 2007.

- Xinwei Sun, Botong Wu, Xiangyu Zheng, Chang Liu, Wei Chen, Tao Qin, and Tie-Yan Liu. Recovering latent causal factor for generalization to distributional shifts. *Advances in Neural Information Processing Systems*, 34, 2021.
- Remi Tachet des Combes, Han Zhao, Yu-Xiang Wang, and Geoffrey J Gordon. Domain adaptation with conditional distribution matching and generalized label shift. *Advances in Neural Information Processing Systems*, 33:19276–19289, 2020.
- Vladimir N Vapnik. An overview of statistical learning theory. *IEEE transactions on neural networks*, 10(5):988–999, 1999.
- Hang Wang, Minghao Xu, Bingbing Ni, and Wenjun Zhang. Learning to combine: Knowledge aggregation for multi-source domain adaptation. In *European Conference on Computer Vision*, pp. 727–744. Springer, 2020.
- Junfeng Wen, Chun-Nam Yu, and Russell Greiner. Robust learning under uncertain test distributions: Relating covariate shift to model misspecification. In *International Conference on Machine Learning*, pp. 631–639. PMLR, 2014.
- Luyu Yang, Yogesh Balaji, Ser-Nam Lim, and Abhinav Shrivastava. Curriculum manager for source selection in multi-source domain adaptation. In *European Conference on Computer Vision*, pp. 608–624. Springer, 2020.
- John R Zech, Marcus A Badgeley, Manway Liu, Anthony B Costa, Joseph J Titano, and Eric Karl Oermann. Variable generalization performance of a deep learning model to detect pneumonia in chest radiographs: a cross-sectional study. *PLoS medicine*, 15(11):e1002683, 2018.
- Kun Zhang, Bernhard Schölkopf, Krikamol Muandet, and Zhikun Wang. Domain adaptation under target and conditional shift. In *International Conference on Machine Learning*, pp. 819–827. PMLR, 2013.
- Kun Zhang, Mingming Gong, and Bernhard Schölkopf. Multi-source domain adaptation: A causal view. In *Twenty-ninth AAAI conference on artificial intelligence*, 2015.
- Han Zhao, Shanghang Zhang, Guanhang Wu, José MF Moura, Joao P Costeira, and Geoffrey J Gordon. Adversarial multiple source domain adaptation. *Advances in neural information processing systems*, 31, 2018.
- Han Zhao, Remi Tachet Des Combes, Kun Zhang, and Geoffrey Gordon. On learning invariant representations for domain adaptation. In *International Conference on Machine Learning*, pp. 7523–7532. PMLR, 2019.

A APPENDIX

Data Details The original PACS (Li et al., 2017) is a multiple domain dataset contains 4 domains, Photo, Artpainting, Cartoon and Sketch, which shares the same seven categories. The KL divergence of label distributions of any two domains in the original PACS is very small, round 0.1. For obtaining the proposed latent covariate shift, we filter the original dataset by re-sampling it, and obtain three new datasets with different the KL divergences of label distributions as depicted by Figure 6. For Terra Incognita (Beery et al., 2018), the label distribution is long-tailed at each domain, and each domain has a different label distribution, which is naturally applicable for our setting. This work use the four domains from the original data, L28, L43, L46 and L7, which shares the same seven categories: bird, bobcat, empty, opossum, rabbit, raccoon, skunk, as depicted by Figure 7

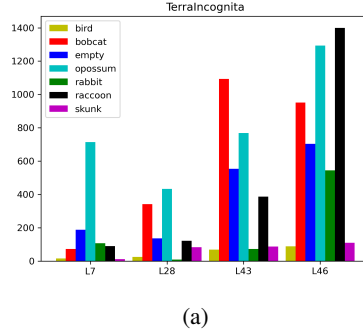


Figure 7: Label distributions of Terra Incognita data used in this work.

Implementation Details For the synthetic data, we used a encoder, *e.g.* 3-layer fully connected network with 30 hidden nodes for each layer, and decoder, *e.g.* 3-layer fully connected network with 30 hidden nodes for each layer. We use 3-layer fully connected network with 30 hidden nodes for prior model. Since this is a ideal environment to verify the proposed method, for hyper-parameters, we set $\beta = 1$ and $\gamma = 0$ to remove the heuristic constraints, and we set $\lambda = 1e - 2$. For the real data, all methods used the same network backbone, ResNet-18 pre-trained on ImageNet. Since it can be challenging to train VAE on high-resolution images, we use extracted features by ResNet-18 as our VAE input. We then use 2-layer fully connected networks as the VAE encoder and decoder, use 2-layer fully connected network for the prior model, use 2-layer fully connected network to transfer \mathbf{n}_c to \mathbf{z}_c . For hyper-parameters, we set $\beta = 4$, $\gamma = 0.1$, $\lambda = 1e - 4$ for the proposed method on all datasets.

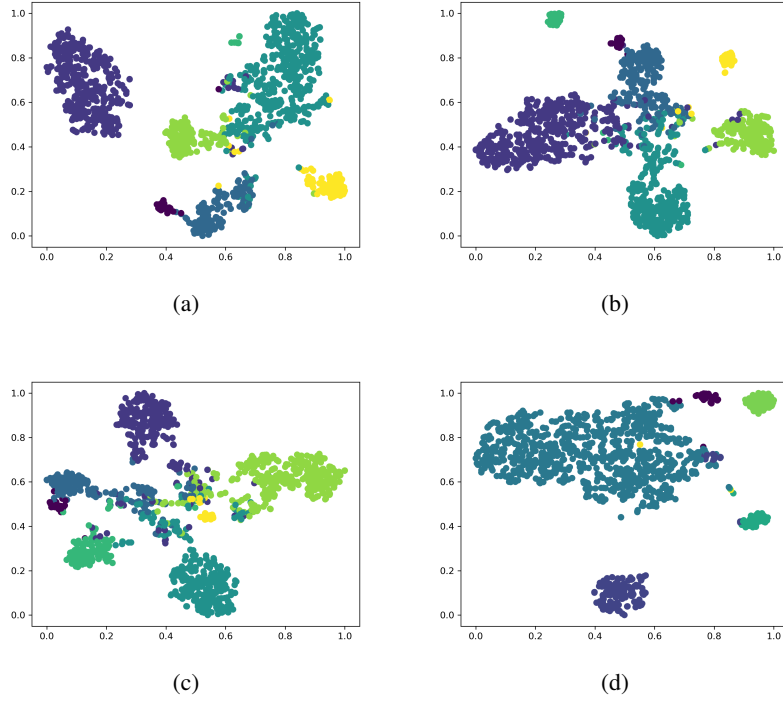


Figure 8: The t-SNE visualizations of learned features \mathbf{n}_c of different domains on the $\rightarrow L7$ task in TerraIncognita. (a) The learned features \mathbf{n}_c in the L28 domain (b) The learned features \mathbf{n}_c in the L43 domain (c) The learned features \mathbf{n}_c in the L46 domain (d) The learned features \mathbf{n}_c in the L7 domain. We can observe that the distribution of learned feature \mathbf{n}_c by the proposed method changes across domains, which is very different with the previous methods based on learning invariant representations.